

Naval Research Laboratory

Washington, DC 20375-5000 NRL Report 9015 November 21, 1986



2

AD-A176 595

Radar Target Detection in Non-Gaussian, Correlated Clutter

B. CANTRELL

*Radar Analysis Branch
Radar Division*

DATA FILE COPY

S DTIC
ELECTE **D**
FEB 04 1987
E

Approved for public release, distribution unlimited.

87 2 4 024



SECURITY CLASSIFICATION OF THIS PAGE

REPORT DOCUMENTATION PAGE				
1a. REPORT SECURITY CLASSIFICATION UNCLASSIFIED		1b. RESTRICTIVE MARKINGS		
2a. SECURITY CLASSIFICATION AUTHORITY		3. DISTRIBUTION / AVAILABILITY OF REPORT Approved for public release; distribution unlimited.		
2b. DECLASSIFICATION / DOWNGRADING SCHEDULE				
4. PERFORMING ORGANIZATION REPORT NUMBER(S) NRL Report 9015		5. MONITORING ORGANIZATION REPORT NUMBER(S)		
6a. NAME OF PERFORMING ORGANIZATION Naval Research Laboratory	6b. OFFICE SYMBOL (If applicable)	7a. NAME OF MONITORING ORGANIZATION		
6c. ADDRESS (City, State, and ZIP Code) Washington, DC 20375-5000		7b. ADDRESS (City, State, and ZIP Code)		
8a. NAME OF FUNDING / SPONSORING ORGANIZATION Office of Naval Research	8b. OFFICE SYMBOL (If applicable) Code 5312	9. PROCUREMENT INSTRUMENT IDENTIFICATION NUMBER		
8c. ADDRESS (City, State, and ZIP Code) Arlington, VA 22217		10. SOURCE OF FUNDING NUMBERS		
		PROGRAM ELEMENT NO. 61153N	PROJECT NO. 021-05-43	TASK NO. WORK UNIT ACCESSION NO. 53-0626-0
11. TITLE (Include Security Classification) Radar Target Detection in Non-Gaussian, Correlated Clutter				
12. PERSONAL AUTHOR(S) Cantrell, Ben				
13a. TYPE OF REPORT Interim	13b. TIME COVERED FROM _____ TO _____	14. DATE OF REPORT (Year, Month, Day) 1986 November 21	15. PAGE COUNT 28	
16. SUPPLEMENTARY NOTATION				
17. COSATI CODES			18. SUBJECT TERMS (Continue on reverse if necessary and identify by block number)	
FIELD	GROUP	SUB-GROUP	-- Detection Radar signal processing Radar	
19. ABSTRACT (Continue on reverse if necessary and identify by block number)				
<p>A new processor for detecting a radar target in correlated, non-Gaussian clutter is obtained. When this processor and a matched filter are excited with this type of data, performance is improved over that of the matched filter alone. The processor is obtained by developing an approximate, multivariate, probability density for the clutter and constructing a Neyman-Pearson test. The processor is then obtained by using an approximation to the likelihood ratio obtained from the Neyman-Pearson test.</p>				
20. DISTRIBUTION / AVAILABILITY OF ABSTRACT <input type="checkbox"/> UNCLASSIFIED/UNLIMITED <input checked="" type="checkbox"/> SAME AS RPT <input type="checkbox"/> DTIC USERS		21. ABSTRACT SECURITY CLASSIFICATION UNCLASSIFIED		
22a. NAME OF RESPONSIBLE INDIVIDUAL Ben H. Cantrell		22b. TELEPHONE (Include Area Code) (202) 767-3406	22c. OFFICE SYMBOL Code 5312	

CONTENTS

INTRODUCTION	1
TRANSFORMATION FORM	2
NONLINEAR SPECIFICATION	2
MULTIVARIATE PROBABILITY DENSITY	3
COVARIANCE MATRIX CALCULATION	4
NEYMAN-PEARSON TEST	9
APPROXIMATE NEYMAN-PEARSON TEST	9
SIMULATION PERFORMANCE OF AN EXAMPLE	12
SUMMARY	18
ACKNOWLEDGMENT	18
REFERENCES	18
APPENDIX A — Locally Optimum Test	19
APPENDIX B — Variance Calculations	21
APPENDIX C — Correlation Coefficient Calculation	23
APPENDIX D — Importance Sampling	25

Accession For	
NTIS GRA&I	<input checked="" type="checkbox"/>
DTIC TAB	<input type="checkbox"/>
Unannounced	<input type="checkbox"/>
Justification	
By _____	
Distribution/	
Availability Codes	
Dist	Avail and/or Special
A-1	



RADAR TARGET DETECTION IN NON-GAUSSIAN, CORRELATED CLUTTER

INTRODUCTION

The optimum filter for detecting radar targets in Gaussian amplitude, distributed, correlated noise, referred to in the radar community as clutter, has been known for many years. This filter is the Wiener or matched filter. This filter can be obtained by using the Neyman-Pearson procedure that maximizes the probability of detection for a given probability of false alarm for a binary hypothesis. In applying this procedure to non-Gaussian, correlated noise, three problems are encountered. First, we seldom know or can easily measure the required multivariate probability density of the noise; second, often there are unknown parameters that must be accounted for in some way; and third, the likelihood ratio obtained in the test sometimes is difficult to simplify. All three of these problems are addressed in this study.

The most difficult problem encountered is obtaining the multivariate probability density of the noise. A procedure for constructing an approximate representation of the multivariate probability density is described by Martinez, Swaszek, and Thomas [1]. The procedure constructs the desired multivariate density from one that can be analytically represented, such as a Gaussian one, by using a nonlinear transform to map the one into the other. The mapping is adjusted so that the marginal distributions and the first two moments of the constructed multivariate distributions are correct. Often these are the only properties of the clutter that can be measured easily. Even though the filter derived from this approximated, multivariate probability density may not be optimum, it may yield a useful result. To test this, the new filter and the Wiener filter can be operated on the same data to see which one yields the best results. If the approximated, multivariate density matches the data better than a Gaussian multivariate density, the new filter should obtain the better performance. In this report, the results of Ref. 1 are modified to include complex numbers to represent radar baseband signals and to provide a suitable form of the nonlinear transformation.

After the multivariate density is found, a Neyman-Pearson test can be obtained. In this test, the unknown parameters are the covariance matrix and the complex signal. The covariance matrix is usually estimated from reference cells and is not considered further. One way of eliminating the unknown signal from the test, as well as simplifying the test, is to use locally optimum tests. Reference 1 describes a test that maximizes the efficacy. Reference 2 describes a test that maximizes the rate of change of the false dismissal probability with respect to signal strength at zero signal strength for a given probability of false alarm. Reference 3 describes a Taylor's series expansion of the likelihood ratio. For additive signal and noise, all three yield the same result. This locally optimum detector is described in Appendix A for the case of complex numbers. However, this test did not yield good performance results. By observing this test, another test based on an approximation to the Neyman-Pearson test was found. This new test, or filter, is independent of the signal amplitude and phase and is fairly easy to implement. Although this test is developed later in this report, the functional flow of the test is shown in Fig. 1. In essence, a mapping is used to transform the random variable to a Gaussian distribution, and then a matched filter is applied to the signal after the nonlinear mapping and after the prewhitening process. This new test is evaluated and presented.

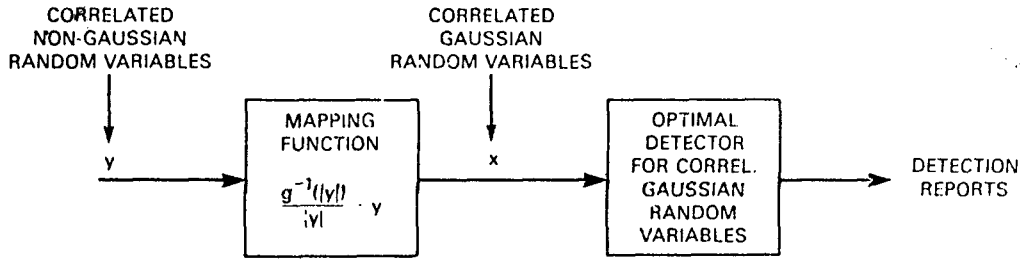


Fig. 1 - Generic signal processor for correlated non-Gaussian inputs

TRANSFORMATION FORM

A zero mean multivariate Gaussian process is defined by the probability density

$$f_N(\mathbf{x}) = \frac{1}{(2\pi)^m |R_x|} \exp \left\{ -\frac{1}{2} \bar{\mathbf{x}}^t R_x^{-1} \mathbf{x} \right\}, \tag{1}$$

where R_x is the $m \times m$ covariance matrix, \mathbf{x} is the random vector of complex numbers of dimension m , m is the number of samples, the bar is the conjugate, and t is the transpose. The multivariate probability density as approximated is defined as $f_N(\mathbf{y})$ where \mathbf{y} is an m -dimensional random vector. The form of $f_N(\mathbf{y})$ will be found later.

The transformations between the random processes \mathbf{x} and \mathbf{y} are defined by

$$y_k = u_k(\mathbf{x}) = \frac{g^{-1}(\sqrt{x_k \bar{x}_k})}{\sqrt{x_k \bar{x}_k}} x_k, \tag{2}$$

$$x_k = v_k(\mathbf{y}) = \frac{g(\sqrt{y_k \bar{y}_k})}{\sqrt{y_k \bar{y}_k}} y_k, \tag{3}$$

where x_k and y_k are components of \mathbf{x} and \mathbf{y} respectively, $g(\)$ is a nonlinear function, and $g^{-1}(\)$ is its inverse. The functions $u_k(\mathbf{x})$ and $v_k(\mathbf{y})$ are components of the random vector $\mathbf{U}(\mathbf{x})$ and $\mathbf{V}(\mathbf{y})$ of dimension m , respectively. Choosing the transformation in this form preserves the phase of the noise and modifies the amplitude. Verifying that the mapping is one to one is done by placing Eq. (3) into Eq. (2).

NONLINEAR SPECIFICATION

Following the procedure in Ref. 1, the nonlinear functions g and g^{-1} can be found by matching the total probability before and after the transformation. Since only g and g^{-1} are defined on the magnitudes of each complex signal individually, the marginal densities of the amplitudes of the signals are used. The nonlinear functions are found from

$$\int_0^{g(|y_k|)} f_N(|x_k|) d|x_k| = \int_0^{|y_k|} f_N(|y_k|) d|y_k|$$

and

$$\int_0^{|x_k|} f_N(|x_k|) d|x_k| = \int_0^{g^{-1}(|x_k|)} f_N(|y_k|) d|y_k|,$$

where

$$|x_k| = \sqrt{x_k \bar{x}_k}$$

and

$$|y_k| = \sqrt{y_k \bar{y}_k}.$$

The marginal amplitude distribution of the Gaussian process is Rayleigh and is given by

$$f_N(|x_k|) = \frac{|x_k|}{\sigma_x^2} \exp\left\{-|x_k|^2 / 2\sigma_x^2\right\},$$

where σ_x^2 is a variance of the underlying Gaussian process. Examples of marginal amplitude distributions for radar clutter are the Weibull and lognormal distributions [4]. The Weibull distribution is given by

$$f_N(|y_k|) = \alpha \ln 2 \left(\frac{|y_k|}{M_y}\right)^{\alpha-1} \exp\left[2 \ln\left(\frac{|y_k|}{M_y}\right)\right]^\alpha,$$

where M_y is the median value and α is the Weibull parameter that ranges from $\sim .5$ to 2 for radar clutter. For $\alpha = 2$, the Weibull reduces to the Rayleigh distribution. The lognormal is given by

$$f_N(|y_k|) = \frac{2}{\sqrt{2\pi} \sigma_l |y_k|} \exp\left\{-\frac{1}{2\sigma_l^2} \left[2 \ln\left(\frac{|y_k|}{M_y}\right)\right]^2\right\},$$

where M_y is the median value and σ_l is the standard deviation of $(\ln|y_k|)^2$. Performing the integrals over the defined marginal densities, the nonlinear functions are found to be

$$g(\sqrt{y_k \bar{y}_k}) = \sqrt{2 \ln 2} \left(\frac{\sqrt{y_k \bar{y}_k}}{M_y}\right)^{\alpha/2}$$

and

$$g^{-1}(\sqrt{x_k \bar{x}_k}) = M_y \left(\frac{\sqrt{x_k \bar{x}_k}}{\sqrt{2 \ln 2}}\right)^{2/\alpha}$$

for the Weibull distribution and

$$g(\sqrt{y_k \bar{y}_k}) = \sqrt{-2 \ln \left[(1/2) \operatorname{erfc} \left\{ \frac{\sqrt{2}}{\sigma_l} \ln \left(\frac{|y_k|}{M_y} \right) \right\} \right]}$$

$$g^{-1}(\sqrt{x_k \bar{x}_k}) = M_y \exp \left\{ \frac{\sigma_l}{\sqrt{2}} \operatorname{erfc}^{-1} \left[2 \exp - \frac{1}{2} |x_k|^2 \right] \right\}$$

for the lognormal. The function erfc is the complimentary error function, erfc^{-1} is its inverse and \ln is the natural logarithm. Without any loss in generality, σ_x is set to 1 in all cases.

MULTIVARIATE PROBABILITY DENSITY

The new approximate multivariate probability density can be written in terms of the multivariate Gaussian and the one-to-one mapping previously defined by using traditional change-of-variable techniques in probability theory. The new density is

$$f_N(y) = f_N(x = V(y)) |J_N| = \frac{|J_N|}{(2\pi)^m |R_N|} \exp \left\{ \frac{1}{2} \bar{V}'(y) R_N^{-1} V(y) \right\}$$

where $|J_N|$ is the Jacobian that is the determinant of a matrix of partial derivatives. A special problem arises in computing the Jacobian for complex numbers, because the $V(y)$ is not analytic with respect to the variables y_k since both y_k and \bar{y}_k appear in the function. Two approaches to circumvent this problem yield the same result. The first is to write y_k in terms of real and imaginary components and determine the Jacobian for $2m$ real functions and variables. An alternate procedure is to treat y_k and \bar{y}_k as independent random variables and $x = V(y)$ and $\bar{x} = \bar{V}(y)$ as independent functions. Now the $2m$ functions are analytic with respect to the $2m$ variables. The latter procedure yields the simplest calculation and is outlined as follows. The Jacobian matrix is written as

$$|J_N| = \begin{vmatrix} J_N(1) & \underline{0} & \underline{0} & \underline{0} \\ \underline{0} & J_N(2) & \underline{0} & \underline{0} \\ \underline{0} & \underline{0} & J_N(3) & \underline{0} \\ \vdots & \vdots & \vdots & \vdots \\ \underline{0} & \underline{0} & \underline{0} & J_N(m) \end{vmatrix}$$

where $J_N(k)$ is a 2×2 matrix given by

$$J_N(k) = \begin{vmatrix} \frac{\partial V_k(y)}{\partial y_k} & \frac{\partial \bar{V}_k(y)}{\partial y_k} \\ \frac{\partial V_k(y)}{\partial \bar{y}_k} & \frac{\partial \bar{V}_k(y)}{\partial \bar{y}_k} \end{vmatrix}$$

and $\underline{0}$ is a 2×2 matrix of zero entries. The Jacobian can be written more simply by

$$|J_N| = \prod_{k=1}^m |J_N(k)|$$

because of the other zero submatrices. After taking the derivatives and evaluating the 2×2 determinants, the Jacobian becomes

$$|J_N| = \prod_{k=1}^m \frac{g(\sqrt{y_k \bar{y}_k}) g'(\sqrt{y_k \bar{y}_k})}{\sqrt{y_k \bar{y}_k}}$$

where $g'(\)$ is the first derivative of g with respect to $|y_k| = \sqrt{y_k \bar{y}_k}$. For Weibull clutter, the Jacobian is

$$|J_N| = \prod_{k=1}^m \frac{\alpha \ln 2}{y_k \bar{y}_k} \left(\frac{\sqrt{y_k \bar{y}_k}}{M_y} \right)^\alpha$$

and for lognormal

$$|J_N| = \prod_{k=1}^m \left[\sqrt{\frac{2}{\pi \sigma^2}} \times \frac{2 \exp(-a^2)}{(y_k \bar{y}_k) \operatorname{erfc}(a)} \right]$$

where

$$a = \sqrt{\frac{2}{\sigma^2}} \ln \left(\frac{\sqrt{y_k \bar{y}_k}}{M_y} \right)$$

COVARIANCE MATRIX CALCULATION

A multivariate probability density function for the non-Gaussian clutter has been constructed, and all functions and parameters have been specified except the covariance matrix R_N . Since the

covariance matrix of the non-Gaussian process is known or measured and the one-to-one mapping defined, the covariance matrix R_x can be computed from R_y by use of the mapping. In this report, the random process y is assumed to be stationary, and its spectrum is assumed to be an even function. For this case, the covariance matrix R_y is real, and any row can be obtained from the first row. This case is valid for all clutter spectrums that have an even symmetry about a mean doppler after this mean doppler shift is removed. The covariance matrices are written in the form of

$$R_y = \sigma_y^2 \begin{bmatrix} 1 & \rho_y(1) & \rho_y(2) & \dots & \rho_y(m-1) \\ \rho_y(1) & 1 & \rho_y(1) & & \\ \rho_y(2) & \rho_y(1) & 1 & & \\ \cdot & & & \cdot & \\ \rho_y(m-1) & & & & 1 \end{bmatrix}$$

and

$$R_x = \sigma_x^2 \begin{bmatrix} 1 & \rho_x(1) & \rho_x(2) & \dots & \rho_x(m-1) \\ \rho_x(1) & 1 & \rho_x(1) & & \\ \rho_x(2) & \rho_x(1) & 1 & & \\ \cdot & & & \cdot & \\ \rho_x(m-1) & & & & 1 \end{bmatrix},$$

where σ_y^2 and σ_x^2 are the variances and $\rho_y(k)$ and $\rho_x(k)$ are the correlation coefficients of the random processes y and x , respectively.

The variance of y can be found in terms of the variance of x , previously set to one, by computing the expected values:

$$\sigma_y^2 = \frac{1}{2} E [y_k \bar{y}_k] = \frac{1}{2} E [u_k(x) \overline{u_k(x)}].$$

The integral equation is

$$\sigma_y^2 = \frac{1}{2} \int_0^\infty \int_0^\infty \frac{[g^{-1}(\sqrt{(x_k^r)^2 + (x_k^i)^2})]^2}{2\pi \sigma_x^2} \exp - \frac{1}{2} \left\{ \frac{(x_k^r)^2 + (x_k^i)^2}{\sigma_x^2} \right\} dx_k^r dx_k^i,$$

where the complex variable x_k is written in terms of its real x_k^r and imaginary x_k^i parts, respectively. Using the change of variable

$$\xi = \sqrt{(x_k^r)^2 + (x_k^i)^2}$$

$$\phi = \tan^{-1} x_k^i / x_k^r$$

and integrating over ϕ , the variance of y_k is

$$\sigma_y^2 = \frac{1}{2\sigma_x^2} \int_0^\infty [g^{-1}(\xi)]^2 \xi \exp - \frac{1}{2} \left\{ \xi^2 / \sigma_x^2 \right\} d\xi.$$

For Weibull clutter and $\sigma_x = 1$,

$$\frac{\sigma_y^2}{M_y^2} = \left\{ \frac{1}{\alpha} \right\} (\ln 2)^{-2/\alpha} \Gamma \left\{ \frac{2}{\alpha} \right\}$$

where $\Gamma(\cdot)$ is the gamma function. For lognormal clutter and $\sigma_x = 1$,

B. CANTRELL

$$\frac{\sigma_y^2}{M_y^2} = (1/2) \exp \{ (\sigma_l / \sqrt{2})^2 \}.$$

Several steps in computing these variances are shown in Appendix B. Short tables of values for σ_y^2 are given in Tables 1 and 2 for Weibull and lognormal clutter, respectively.

Table 1 — Values of σ_y^2/M_y^2 Given Values of α for Weibull Clutter

α	σ_y^2/M_y^2
0.50	51.985162
0.75	5.331132
1.00	2.081369
1.25	1.284905
1.50	0.970471
1.75	0.812625
2.00	0.721348

Table 2 — Values of σ_y^2/M_y^2 Given Values of σ_l for Lognormal Clutter

σ_l	σ_y^2/M_y^2
0.8	0.6886
0.9	0.497
1.0	0.8244
1.1	0.9156
1.3	1.1640
1.5	1.5401
1.7	2.1209

The correlation coefficient $\rho_y(k)$ can be found in terms of the correlation coefficient $\rho_x(k)$ by

$$\rho_y(k) = \frac{1}{2} \frac{E[y_l \bar{y}_{l+k}]}{\sigma_y^2} = \frac{1}{2} \frac{E[u_l(\mathbf{x}) \bar{u}_{l+k}(\mathbf{x})]}{\sigma_y^2}$$

for $k = 1, \dots, (m-1)$. Since the complex portion of $\rho_y(k)$ is zero under our assumption of an even spectrum and

$$E[y_l \bar{y}_{l+k}] = E[y_l y_{l+k}] = E[u_l(\mathbf{x}) \bar{u}_{l+k}(\mathbf{x})] = E[u_l(\mathbf{x}) u_{l+k}(\mathbf{x})],$$

then

$$\rho_y(k) = \frac{1}{\sigma_y^2} \int_{-\infty}^{\infty} \int_{-\infty}^{\infty} \int_{-\infty}^{\infty} \int_{-\infty}^{\infty} \frac{x_l' g^{-1}(\sqrt{(x_l')^2 + (x_l)^2}) x_{l+k}' g^{-1}(\sqrt{(x_{l+k}')^2 + (x_{l+k})^2})}{\sqrt{(x_l')^2 + (x_l)^2} \sqrt{(x_{l+k}')^2 + (x_{l+k})^2}} \times f_N(x_l', x_l, x_{l+k}', x_{l+k}) dx_l' dx_l dx_{l+k}' dx_{l+k},$$

where

$$f_N(x_l', x_l, x_{l+k}', x_{l+k}) = \frac{1}{4\pi^2 \sigma_x^2 (1 - \rho_x^2(k))} \times \exp - \left\{ \frac{(x_l')^2 + (x_{l+k}')^2 - 2\rho_x(k) x_l' x_{l+k}'}{2\sigma_x^2 (1 - \rho_x^2(k))} \right\} \times \exp - \left\{ \frac{(x_l)^2 + (x_{l+k})^2 - 2\rho_x(k) x_l x_{l+k}}{2\sigma_x^2 (1 - \rho_x^2(k))} \right\}.$$

Using the change of variable,

$$\xi_l = \sqrt{(x_l')^2 + (x_l)^2} \quad \xi_{l+k} = \sqrt{(x_{l+k}')^2 + (x_{l+k})^2}$$

$$\tan \theta_l = x_l' / x_l \quad \tan \theta_{l+k} = x_{l+k}' / x_{l+k},$$

yields the new integral

$$\rho_y(k) = \int_0^\infty \int_0^\infty \frac{\xi_l \xi_{l+k} g^{-1}(\xi_l) g^{-1}(\xi_{l+k})}{4\pi^2 \sigma_x^4 (1 - \rho_x^2(k))} \exp - \left[\frac{\xi_l^2 + \xi_{l+k}^2}{2\sigma_x^2 (1 - \rho_x^2(k))} \right] \int_0^{2\pi} \int_0^{2\pi} \cos \theta_l \cos \theta_{l+k} \\ \times \exp \left[\frac{2\rho_x(k) \xi_l \xi_{l+k} \cos(\theta_l - \theta_{l+k})}{\sigma_x^2 (1 - \rho_x^2(k))} \right] d\theta_l d\theta_{l+k} d\xi_l d\xi_{l+k}.$$

Changing variables again by

$$\theta_d = \theta_l - \theta_{l+k}$$

$$\theta_s = \theta_l + \theta_{l+k}$$

and integrating over θ_d and θ_s , we obtain

$$\rho_y(k) = \frac{1}{\sigma_v^2} \int_0^\infty \int_0^\infty \frac{\xi_l \xi_{l+k} g^{-1}(\xi_l) g^{-1}(\xi_{l+k})}{\sigma_x^2 (1 - \rho_x^2(k))} I_1 \left[\frac{\rho_x(k) \xi_l \xi_{l+k}}{(1 - \rho_x^2(l)) \sigma_x^2} \right] \\ \times \exp - \left[\frac{\xi_l^2 + \xi_{l+k}^2}{2\sigma_x^2 (1 - \rho_x^2(k))} \right] d\xi_l d\xi_{l+k},$$

where $I_1(\cdot)$ is the modified Bessel function of the first kind and first order.

For Weibull clutter, the required integration can be carried out in closed form, and the result is

$$\rho_y(k) = \left[\frac{\alpha}{2} \right] \rho_x(k) (1 - \rho_x^2(k))^{\left[\frac{2}{\alpha} + 1 \right]} \left[\Gamma' \left[\frac{1}{\alpha} + \frac{3}{2} \right] / \Gamma' \left[\frac{2}{\alpha} \right] \right] \\ \times F \left[\left[\frac{1}{\alpha} + \frac{3}{2} \right], \left[\frac{1}{\alpha} + \frac{3}{2} \right], 2, \rho_x^2(k) \right],$$

where $F(\cdot, \cdot, \cdot, \cdot)$ is the hypergeometry function that can be written in the infinite series

$$F(\nu, \mu, \gamma, \rho_x^2(k)) = 1 + \frac{\nu\mu}{\gamma \cdot 1} \rho_x^2(k) + \frac{\nu(\nu+1)\mu(\mu+1)}{\gamma(\gamma+1) \cdot 1 \cdot 2} (\rho_x^2(k))^2 \\ + \frac{\nu(\nu+1)(\nu+2)\mu(\mu+1)(\mu+2)}{\gamma(\gamma+1)(\gamma+2) \cdot 1 \cdot 2 \cdot 3} (\rho_x^2(k))^3 + \dots$$

where the region of convergence is $\rho_x^2(k) < 1$. The details of the integration are outlined in Appendix C. For $\alpha = 2$, which is the case of Rayleigh clutter,

$$F(2, 2, 2, \rho_x^2(k)) = \sum_{i=0}^{\infty} (i+1) [\rho_x^2(k)]^i = \frac{1}{(1 - \rho_x^2(k))^2}.$$

$\Gamma(2) = \Gamma(1) = 1$, $\rho_v(k) = \rho_x(k)$, and the transformation is $y = x$. No closed-form expression relating $\rho_v(k)$ to $\rho_x(k)$ for lognormal clutter is found. The relationship is found by using a Monte Carlo simulation. Numerical values for $\rho_v(k)$ as a function of $\rho_x(k)$ are given in Tables 3 and 4 for Weibull and lognormal clutter, respectively.

NEYMAN-PEARSON TEST

The classic solution for optimally detecting a signal in noise is the Neyman-Pearson test. Specifically, the problem is formulated as a binary hypothesis test

$$\begin{aligned}
 H_0 & \quad \mathbf{y} = \mathbf{n} \\
 H_1 & \quad \mathbf{y} = \mathbf{n} + \mathbf{s}.
 \end{aligned}$$

The hypothesis of the measurement \mathbf{y} containing only noise \mathbf{n} is H_0 and the hypothesis that the measurement \mathbf{y} contains noise plus signal \mathbf{s} is H_1 . The optimal procedure for detection given a fixed false alarm rate is the likelihood ratio function

$$\lambda_{np} = \frac{f_{S+N}(\mathbf{y})}{f_N(\mathbf{y})},$$

where $f_{S+N}(\mathbf{y})$ is the probability density of \mathbf{y} given signal plus noise, and $f_N(\mathbf{y})$ is the defined probability density of \mathbf{y} given noise only. Since $f_{S+N}(\mathbf{y})$ can be expressed in terms of $\mathbf{y} = \mathbf{n} + \mathbf{s}$, the likelihood function becomes

$$\lambda_{np} = \frac{\frac{|J_{N+S}|}{(2\pi)^m |R_x|} \exp \frac{1}{2} \left\{ \overline{V'(y-s)} R_x^{-1} V(y-s) \right\}}{\frac{|J_N|}{(2\pi)^m |R_y|} \exp \frac{1}{2} \left\{ \overline{V'(y)} R_y^{-1} V(y) \right\}}$$

where

$$|J_{N+S}| = \prod_{i=1}^m \frac{g'(|y_i - s_i|) g(|y_i - s_i|)}{|y_i - s_i|}$$

and s_i are components of the signal \mathbf{s} . The signal \mathbf{s} is written as

$$\mathbf{s} = S e^{-j\phi_s} \hat{\mathbf{s}},$$

where S is the signal magnitude, ϕ_s is its phase, and $\hat{\mathbf{s}}$ is its steering vector. In radar applications, ϕ_s represents the pulse-to-pulse phase rotation due to doppler shift of the target. Since ϕ_s is unknown, a bank of filters is usually constructed. One example is for m steering vectors whose complex values are elements of an m -point discrete Fourier transform. The clutter ratio per pulse is defined to be

$$(S/C) = \frac{S^2}{2\sigma_s^2}$$

Because the amplitude and phase is unknown, the likelihood ratio function is not in closed form. Several procedures are possible. One procedure is to assume a range of phase values and average the likelihood ratio function over them. However, in this case, the performance is degraded. Another possible approach is to use locally optimal detectors as discussed in [1]. This approach yielded poor performance for the examples considered. Finally, the likelihood ratio function can be approximated using an approximation. The resulting test is independent of amplitude and phase. The test is described next and its performance for several examples is evaluated.

APPROXIMATE NEYMAN-PEARSON TEST

Many radar problems involve clutter which is highly correlated in time and space. The clutter is modeled as a Gaussian process with a correlation matrix R_c and a mean vector \mathbf{m}_c . The signal \mathbf{s} is assumed to be uncorrelated with the clutter and is modeled as a Gaussian process with a correlation matrix R_s and a mean vector \mathbf{m}_s . The total correlation matrix R_x and mean vector \mathbf{m}_x are given by

ter

2.0
0
.1
.2
.3
.4
.5
.6
.7
.8
.9
.91
.92
.93
.94
.95
.96
.97
.98
.99

$$v_k(y-s) = v_k(y) - c v_k(s)$$

or

$$v_k(y-s) = \frac{g(\sqrt{y_k \bar{y}_k})}{\sqrt{y_k \bar{y}_k}} y_k - c \frac{g(\sqrt{\hat{s}_k \bar{s}_k})}{\sqrt{\hat{s}_k \bar{s}_k}} \hat{s}_k e^{-j\phi_s}$$

is suggested where c is a proportionality constant. The reason why this approximation may be good follows. From pulse to pulse (k to $k+1$), the measurements y_k and y_{k+1} are nearly equal for strongly correlated noise. If the measurement y_k is fixed for all k and the signal phase varies from zero to 2π , the resultant signal looks much like a target making one revolution in doppler space for a high prf waveform when strong clutter is present. The real and imaginary parts $v_k(y-s)$ are given in Figs. 2 and 4 and Figs. 3 and 5 for two examples, respectively. Both the true and approximate values of $v_k(y-s)$ are given. The first example shown in Figs. 2 and 3 is a case when the clutter level is 30 dB above the signal and the initial and fixed phase of the clutter is 0° . The second example shown in Figs. 4 and 5 is the same as that shown in Figs. 2 and 3 except the clutter phase is 45° . In Figs. 2 and 3 the phase matches exactly while the magnitude differs slightly. In Figs. 4 and 5, the phase and amplitude of the true and approximate solution is nearly the same.

Assuming the approximation for $V(y-s)$ is valid, the Neyman-Pearson test using this approximation becomes

$$\ln \lambda_{np} = \frac{1}{2} c \left[\overline{V'(s)} R_N^{-1} V(y) \right] + \frac{1}{2} c \left[\overline{V'(s)} R_N^{-1} V(y) \right]' \\ + c^2 \left[\overline{V'(s)} R_N^{-1} V(s) \right]^2 + \ln(|J_{S+N}|) - \ln(|J_N|).$$

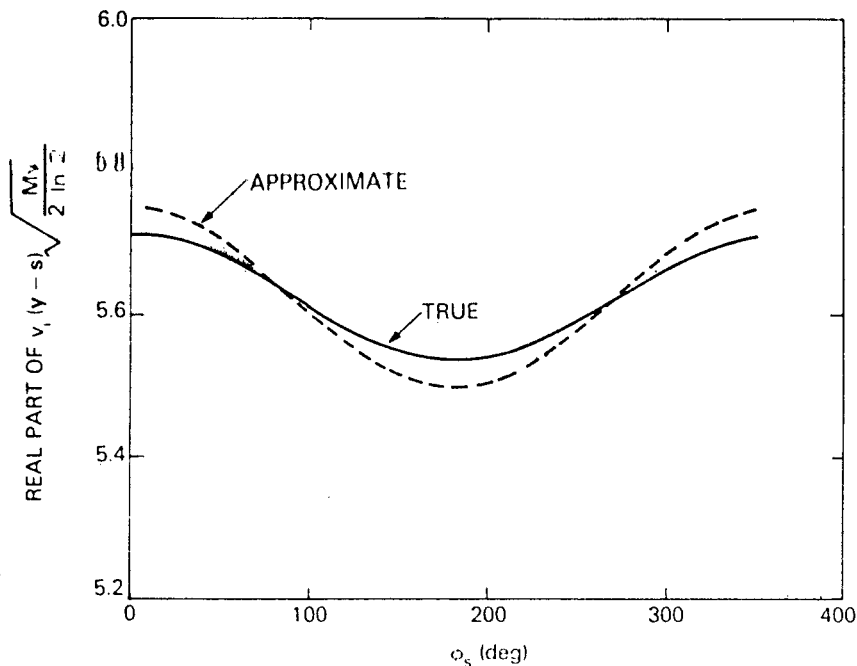


Fig. 2 - Comparison of true and approximate values of the real part of $v_k(y-s)$ as a function of the phase of v_k given $S = 1$, $\phi_{v_k} = 0$, $|v_k| = 31.6$, $c = 125$, and $\alpha = 1$.

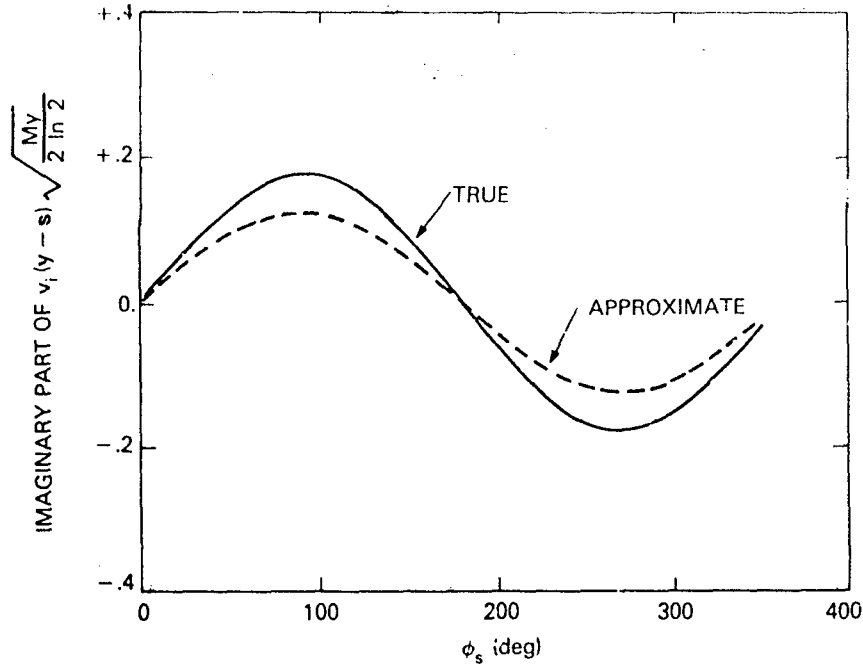


Fig. 3 - Comparison of true and approximate values of the imaginary part of $v_i(y-s)$ as a function of the phase of y_i given $S = 1$, $\phi_{y_i} = 0$, $|y_i| = 31.6$, $c = .125$, and $\alpha = 1$

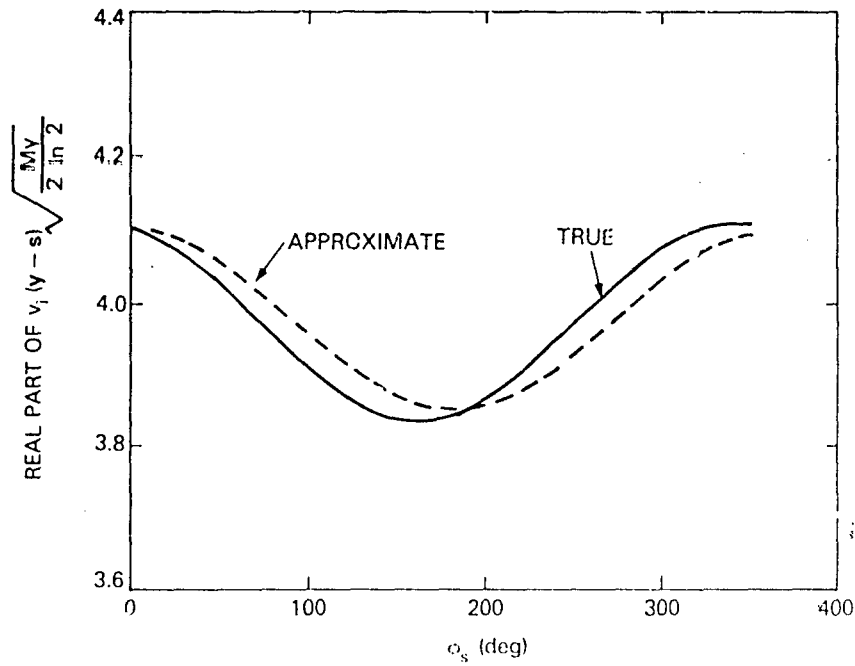


Fig. 4 - Comparison of true and approximate values of the real part of $v_i(y-s)$ as a function of the phase y_i given $S = 1$, $\phi_{y_i} = 45^\circ$, $|y_i| = 31.6$, $c = .125$, and $\alpha = 1$

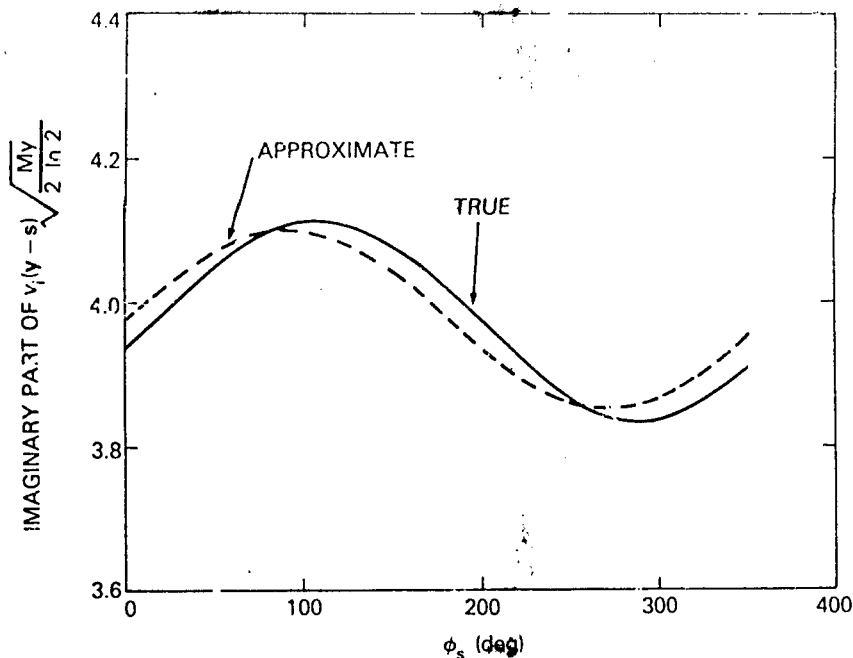


Fig. 5 — Comparison of true and approximate values of the imaginary part of $v_i(y-s)$ as a function of the phase of y_i given $|\hat{s}| = 1$, $\phi_{y_i} = 45^\circ$, $|y_i| = 31.6$, $c = .125$, and $\alpha = 1$

The signal energy and c can be absorbed in the threshold. The Jacobians under the assumption are almost equal and consequently are assumed to cancel. The phase ϕ_s is still unknown. However, if the magnitude of the resultant is computed instead of the real part, only a little loss is incurred. The same technique is used to obtain the matched filter results. Consequently, the Neyman-Pearson test is approximated by

$$\lambda_a = \left| \overline{V'(s)} R_x^{-1} V(y) \right|$$

Since the signal phase can be easily removed from this expression, the approximate test is

$$\lambda_a = \left| \overline{V'(\hat{s})} R_x^{-1} V(y) \right|$$

leaving the test in terms of the steering vector \hat{s} , the data y , the covariance R_x , and the mapping function $V(\cdot)$. The matched filter given by

$$\lambda_{mf} = \left| \hat{s}^T R_y^{-1} y \right|$$

is of similar form. Comparing λ_a and λ_{mf} , the data vector y is mapped into $V(y)$, the signal steering vector \hat{s} is mapped into $V(\hat{s})$, and the covariance R_y is mapped into R_x . All the mappings are defined by the requirements on the marginal density functions.

SIMULATION PERFORMANCE OF AN EXAMPLE

The performance of the detector is evaluated by using data samples obtained from the constructed multivariate density of the clutter. The performance curves are defined as probability-of-detection vs signal-to-noise ratio given a fixed probability of false alarm for various problem conditions. The performance of the approximate Neyman-Pearson test is compared to that of the matched filter and square-law integrator defined by

$$\lambda_{st} = \sum_{i=1}^m |y_i|^2$$

for the same data obtained from the constructed density.

The clutter samples are constructed as follows. A zero mean independent Gaussian process with m samples is defined by the vector \mathbf{z} . A linear transformation L is defined on \mathbf{z} to obtain \mathbf{x} by

$$\mathbf{x} = L\mathbf{z}.$$

The transformation L is defined to be a lower triangular matrix such that it is a factor of R_x defined by

$$R_x = LL'.$$

In the example to be solved subsequently,

$$L = \begin{bmatrix} \sigma_x & 0 \\ \sigma_x \rho_x(1) & \sigma_x \sqrt{1 - \rho_x^2(1)} \end{bmatrix}$$

for $m = 2$. Consequently,

$$R_x = E[\bar{\mathbf{x}}\bar{\mathbf{x}}'] = LE[\bar{\mathbf{z}}\bar{\mathbf{z}}']L' = LL'.$$

The data samples are then computed by

$$\mathbf{y} = U(L\mathbf{z})$$

under H_0 and

$$\mathbf{y} = U(L\mathbf{z} + S e^{-j\phi_s} \hat{\mathbf{s}})$$

under H_1 , where $U(\cdot)$ was previously defined as the transformation between \mathbf{y} and \mathbf{x} .

The example uses $m = 2$ samples. The clutter is Weibull distributed with $\alpha = 1, 1.5, \text{ and } 2$, or lognormal with $\sigma_l = 0.8, 1, \text{ and } 1.5$. In this example, $M_y = 1$, $\sigma_x = 1$, $\rho_x(1) = 0.98$, ϕ_s is arbitrary, and the steering vector is

$$\hat{\mathbf{s}}' = [(1/\sqrt{2} + j0) \quad (0 + j1/\sqrt{2})]$$

which represents a 90° phase rotation of the signal between two pulses. The values of σ_l^2 and $\rho_x(1)$ are found in Tables 1 through 4. The three detectors being compared are the approximate Neyman-Pearson test

$$\lambda_a = \left| \overline{\mathbf{V}'(\hat{\mathbf{s}})} R_x^{-1} \mathbf{V}(\mathbf{y}) \right|,$$

the matched filter

$$\lambda_{mf} = \left| \overline{\mathbf{s}'^t} R_y^{-1} \mathbf{y} \right|,$$

and the square-law detector

$$\lambda_{st} = \overline{\mathbf{y}}^t \mathbf{y}.$$

The thresholds of the detectors are denoted by λ_a^* , λ_{mf}^* , and λ_{st}^* . Figures 6 and 7 are block diagrams for the data generation and three processors to be compared for the two sample examples.

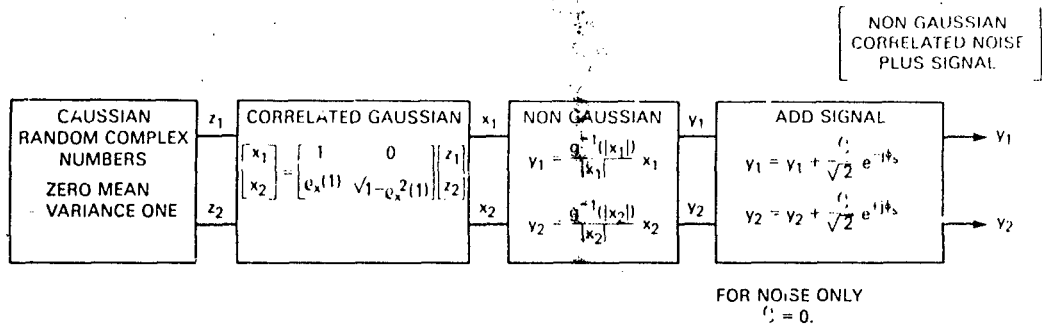


Fig. 6 — Block diagram of data generation used to determine performance characteristics by simulation for two-pulse example

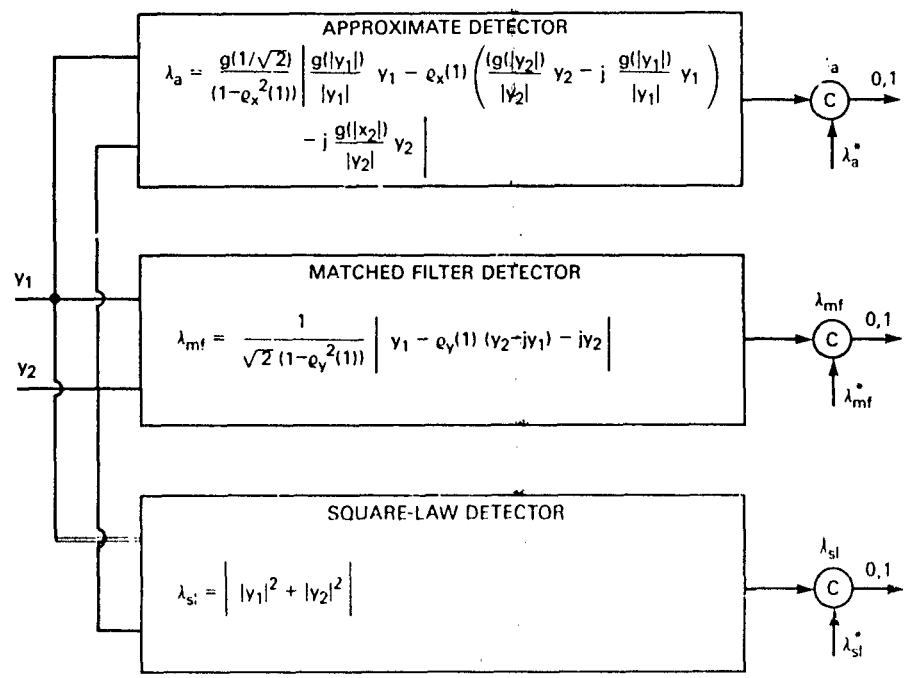


Fig. 7 — Block diagram of three processors to be compared for two-pulse example

The probability of false alarm p_{fa} vs threshold is computed using Monte Carlo simulation techniques. Random samples of y under H_0 are generated. A normalized histogram of the number of samples having values in a small interval for each detector are found. After many trials, a curve of the probability density of the output of each detector vs λ_a , λ_{mf} , and λ_{sl} for each of the three detectors is obtained. The probability of false alarm is defined as the sum of all values of the density from λ_a^* , λ_{mf}^* , and λ_{sl}^* for each filter to infinity. For small values of the probability of false alarm, an importance sampling technique is used. This procedure distorts the generation of random samples so that more false alarms occur than should and then compensates for this in the weightings used in the generation of the histogram. This technique is outlined in Appendix D.

Using the Monte Carlo simulation, the probability of false alarms vs thresholds are shown in Table 5 for Weibull clutter of parameters $\alpha = 1, 1.5, 2.5$ and the three detectors. Several points should be noted. First, the threshold values for a given probability of false alarm for all three values of α for the approximate detector are the same, because the data entering the processor is really x , which is independent of α . However, even though the thresholds are the same, the probability of detection will be different in all three cases because of the way the signal and noise interact. For $\alpha = 2$, the matched filter and the approximate filter are the same detector except for the constant multiplier of $\sqrt{2} \ln 2$. A similar table for lognormal clutter is shown in Table 6.

Table 5 — Probability of False Alarm vs Thresholds for Weibull Clutter

	α	P_{fa}						
		10^{-1}	10^{-2}	10^{-3}	10^{-4}	10^{-5}	10^{-6}	10^{-7}
Approximate filter λ_a	1.0	18.0	25.6	31.2	36.1	40.3	44.2	47.5
	1.5	18.0	25.6	31.2	36.1	40.3	44.2	47.5
	2.0	18.0	25.6	31.2	36.1	40.3	44.2	47.5
Matched filter λ_{mf}	1.0	10.2	19.2	27.9	37.2	46.2	55.2	63.9
	1.5	13.0	19.8	25.6	30.6	35.6	40.0	44.2
	2.0	14.5	20.7	25.2	29.2	32.6	35.7	38.3
Square-law λ_{sl}	1.0	24.0	90.0	195.0	357.0	543.0	786.0	1080.0
	1.5	10.0	25.0	43.0	64.0	84.0	108.0	133.0
	2.0	6.6	13.5	19.8	26.7	33.0	39.9	46.5

Table 6 — Probability of False Alarm vs Thresholds for Lognormal Clutter

	σ_1	P_{fa}						
		10^{-1}	10^{-2}	10^{-3}	10^{-4}	10^{-5}	10^{-6}	10^{-7}
Approximate filter λ_a	.8	18.0	25.6	31.2	36.1	40.3	44.2	47.5
	1.0	18.0	25.6	31.2	36.1	40.3	44.2	47.5
	1.5	18.0	25.6	31.2	36.1	40.3	44.2	47.5
Matched filter λ_{mf}	.8	19.5	33.0	42.7	52.9	57.3	62.1	76.6
	1.0	16.6	26.6	35.8	49.8	69.7	90.7	114.5
	1.5	10.8	23.4	43.0	73.2	120.0	178.0	247.0
Square-law λ_{sl}	.8	5.8	13.2	23.8	39.6	59.2	88.8	129.4
	1.0	7.8	20.6	44.4	80.8	139.0	232.0	343.0
	1.5	14.4	66.0	210.0	515.0	1160.0	2520.0	4500.0

The performance of the detectors are compared by observing the probability of detection vs signal-to-noise ratio for a fixed probability of false alarm. The probability of detection is computed using a Monte Carlo simulation. The fraction of time the detector output exceeds the threshold for a set of randomly generated samples is computed. This number is the probability of detection.

Performance results are shown in Figs. 8, 9, and 10 for Weibull parameters of $\alpha = 1.0, 1.5,$ and 2.0 respectively. In all cases, the probability of false alarm is 10^{-7} . Figure 8 shows that the approximate detector performs better than the matched filter, which performs better than the square-law detector. The subclutter visibility is defined as the difference between the square-law detector and either the matched filter or the approximate detector in signal-to-clutter ratio (in dB) for a given probability of detection. For example, for a probability of detection of 0.5, the subclutter visibility for the matched filter detector is ~ 18 dB, and for the approximate detector it is ~ 30 dB. Figure 9 shows that the performance of the matched filter and square-law detectors improves over those shown in Fig. 8, while the approximate detector performance degrades a little. The reason for this is that the clutter is less spiky in Fig. 9 and the thresholds can be lowered significantly for the matched filter and square-law detectors. Figure 10 shows that the approximate and the matched filter detector yield the same performance because the detectors are identical for Gaussian noise. The square-law detector performance is about the same as the square-law detector for a single pulse when Gaussian noise is present because of the heavy correlation between the two pulses. Figures 11, 12, and 13 show similar results for lognormal clutter.

R. CANTRELL

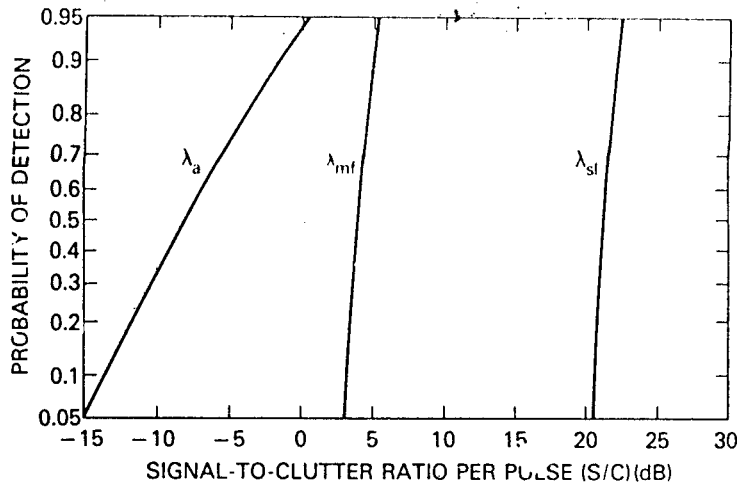


Fig. 8 - Detector operating characteristics for Weibull clutter where $\alpha = 1.0$ and $p_{fa} = 10^{-7}$

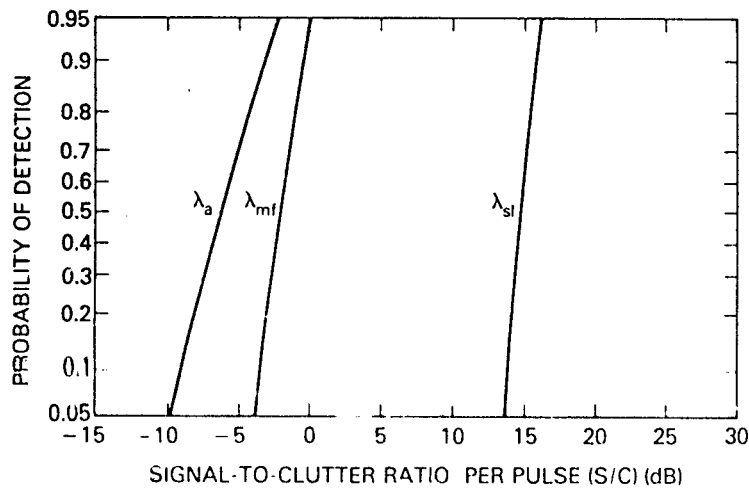


Fig. 9 - Detector operating characteristics for Weibull clutter where $\alpha = 1.5$ and $p_{fa} = 10^{-7}$

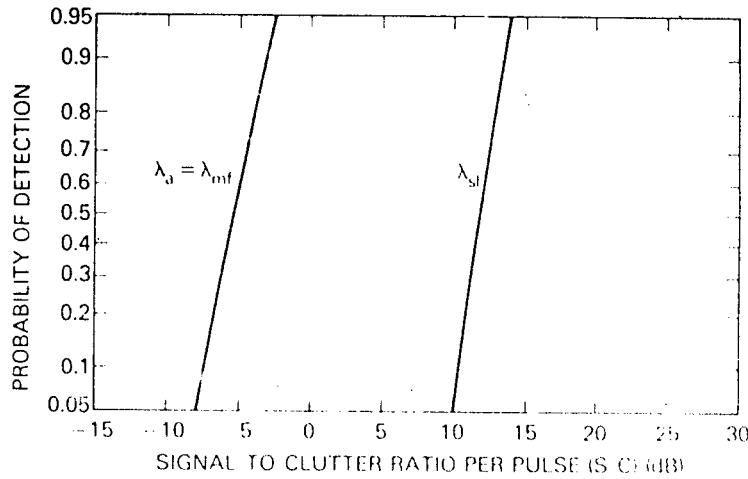


Fig. 10 - Detector operating characteristics for Weibull clutter where $\alpha = 2.0$ and $p_{fa} = 10^{-7}$

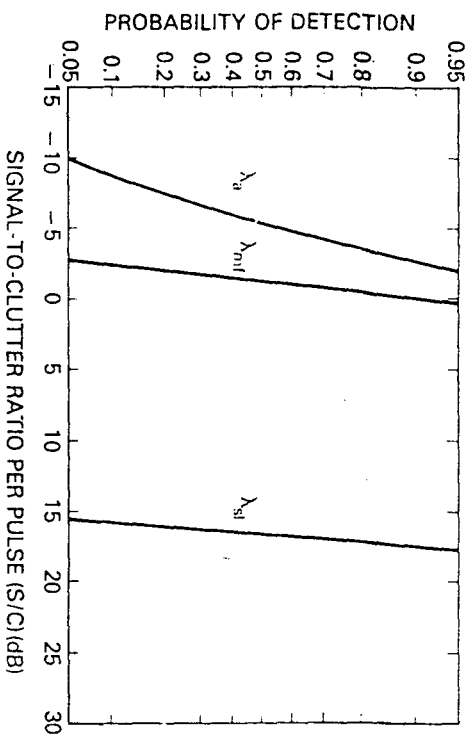


Fig. 11 - Detector operating characteristics for lognormal clutter where $\sigma_l = 1.5$ and $p/a = 10^{-7}$

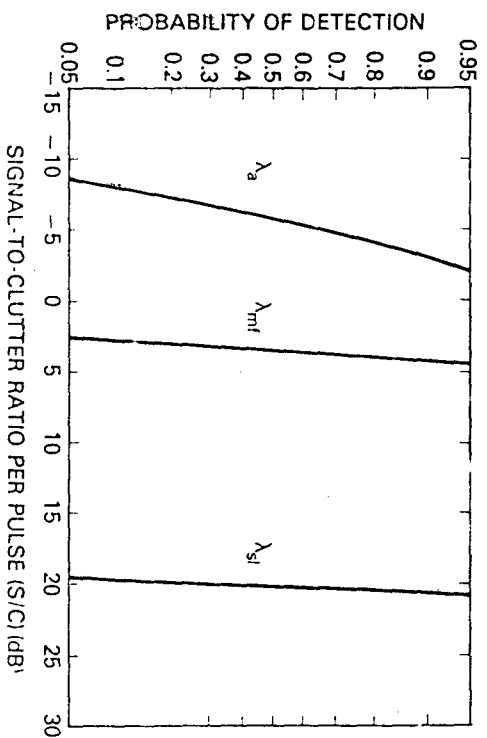


Fig. 12 - Detector operating characteristics for lognormal clutter where $\sigma_l = 1.0$ and $p/a = 10^{-7}$

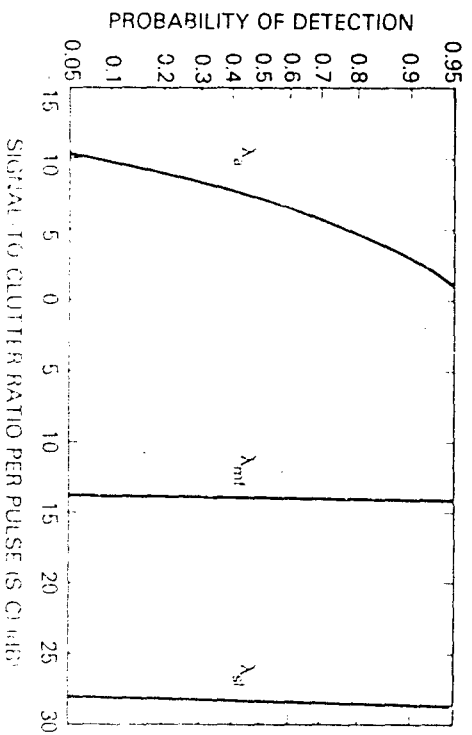


Fig. 13 - Detector operating characteristics for lognormal clutter where $\sigma_l = 1.0$ and $p/a = 10^{-7}$

B. CANTRELL

The approximate detector performed much better than the matched filter detector when the clutter was spiky; performance became nearly the same as the clutter approached a Gaussian distribution. However, the usefulness of the approximate detector must wait until it is evaluated on sets of real data where the true multivariate distributions are unknown and are approximated using the techniques described.

SUMMARY

A procedure to detect a target in non-Gaussian correlated clutter is obtained. Since the multivariate probability density is unknown, an approximate one is constructed. The constructed density matches the true density in the marginals and first two moments. The mapping required and the relationships between the variances are found for both the Weibull and the lognormal clutter distributions. The relationship between the correlation coefficients for Weibull clutter is found, and a similar one for the lognormal distribution is determined by simulation.

An approximate solution is obtained for the Neyman-Pearson test by using the constructed multivariate distributions. Its form is similar to that of a matched filter. In the new coordinates, after a nonlinear operation, the matched filter and the new detector are identical in form. For the examples shown, the new approximate detector performs better than the matched filter when the clutter is spiky and correlated. As the clutter becomes more Gaussian, the two detectors' performance approach one another. Although the true performance of this technique cannot really be assessed until it is applied to real data, it should perform better than the matched filter because the densities used in obtaining it should much more closely describe the data than the Gaussian one does.

ACKNOWLEDGMENT

I thank Dr. Bill Gordon of NRL for helping me to compute both the Jacobian and the simplifying derivative of the locally optimum test found in Appendix A with complex numbers. The forms shown are much simpler than the forms I first used involving real and imaginary parts even though the results are the same using both methods of computation.

REFERENCES

1. A.B. Martinez, P.F. Swaszek, and J.B. Thomas, "Locally Optimal Detection in Multivariate Non-Gaussian Noise," *IEEE Trans. Inf. Theory* **IT-30**(6) 815-822 (1984).
2. J. Capon, "On the Asymptotic Efficiency of Locally Optimum Detectors," *IRE Trans. Inf. Theory* **IT-7**(2) 67-71 (1961).
3. J.J. Sheehy, "Optimum Detection of Signals in Non-Gaussian Noise," *J. Acoust. Soc. Am.* **63**(1) 81-90, (1978).
4. M.I. Skolnik, *Introduction to Radar Systems* (McGraw-Hill, 1980).
5. I.S. Gradshteyn and I.M. Ryzhik, *Table of Integrals, Series, and Products* (Academic Press, New York, 1965).
6. F.S. Hillier and G.J. Lieberman, *Introduction to Operations Research* (Holden-Day, San Francisco, 1967), pp. 457-459.
7. B.H. Cantrell and G.V. Trank, "Corrections to "Angular Accuracy of a Scanning Radar Employing a Two Pole Filter," *IEEE Trans. Aerospace and Electronic Systems* **AES-10**(6) 878-881 (1974).

Appendix A LOCALLY OPTIMUM TEST

The locally optimum test defined by Capon [A1] is

$$\lambda_{lo} = \left. \frac{\partial \lambda_{np}}{\partial S} \right|_{S=0}$$

This is also the first term in a Taylor's series taken about zero signal strength. For real variables, the test defined by Martinez [A2] is equivalent to these other tests for additive signal and noise and is of the form

$$\lambda_{lo} = \text{signal vector transpose} \cdot \text{gradient of } f_N(\mathbf{y})$$

Either form can be used as long as all terms and expressions involving complex numbers are converted to real and imaginary parts in the second procedure. Alternately, using Capon's form, basic definitions of total derivatives, and by treating y_i and \bar{y}_i as independent analytic variables, the locally optimum detector can be most easily computed by

$$\lambda_{lo} = e^{+j\phi_s} \hat{\mathbf{s}}^t \nabla_{\mathbf{y}} (f_N(\mathbf{y})) + e^{-j\phi_s} \hat{\mathbf{s}}^t \nabla_{\bar{\mathbf{y}}} (f_N(\mathbf{y})),$$

where $\nabla_{\mathbf{y}}$ and $\nabla_{\bar{\mathbf{y}}}$ are the gradients defined by

$$\nabla_{\mathbf{y}} = \begin{bmatrix} \frac{\partial}{\partial y_1} \\ \frac{\partial}{\partial y_2} \\ \vdots \\ \frac{\partial}{\partial y_N} \end{bmatrix} \quad \text{and} \quad \nabla_{\bar{\mathbf{y}}} = \begin{bmatrix} \frac{\partial}{\partial \bar{y}_1} \\ \frac{\partial}{\partial \bar{y}_2} \\ \vdots \\ \frac{\partial}{\partial \bar{y}_N} \end{bmatrix}$$

For the Neyman-Pearson test, the locally optimum detector is

$$\lambda_{lo} = \left[\frac{e^{+j\phi_s}}{4} \right] (\hat{\mathbf{s}}^t) \left[\bar{\mathbf{A}}(\mathbf{y}) \mathbf{R}_v^{-1} \bar{\mathbf{V}}(\mathbf{y}) + \bar{\mathbf{B}}(\bar{\mathbf{y}}) \mathbf{R}_v^{-1} \mathbf{V}(\mathbf{y}) - \bar{\mathbf{D}}(\mathbf{y}) \right] \\ + \left[\frac{e^{-j\phi_s}}{4} \right] (\bar{\mathbf{s}}^t) \left[\mathbf{A}(\mathbf{y}) \mathbf{R}_v^{-1} \mathbf{V}(\mathbf{y}) + \mathbf{B}(\mathbf{y}) \mathbf{R}_v^{-1} \bar{\mathbf{V}}(\bar{\mathbf{y}}) - \mathbf{D}(\mathbf{y}) \right]$$

This test still has the unknown phase ϕ_s . However, it is a form similar to the matched filter that also has an unknown phase. In that case as well as the case here, we can compute and use

$$|\lambda_{lo}| = \left| (\hat{\mathbf{s}}^t) \left[\mathbf{A}(\mathbf{y}) \mathbf{R}_v^{-1} \mathbf{V}(\mathbf{y}) + \mathbf{B}(\mathbf{y}) \mathbf{R}_v^{-1} \bar{\mathbf{V}}(\bar{\mathbf{y}}) - \mathbf{D}(\mathbf{y}) \right] \right|$$

B. CANTRELL

with little loss in detection performance. The matrixes are given by

$$\mathbf{A}(\mathbf{y}) = \nabla_{\mathbf{y}} (U'(\mathbf{y}))$$

$$\mathbf{B}(\mathbf{y}) = \nabla_{\mathbf{y}} (V'(\mathbf{y}))$$

and the vector is

$$D(\mathbf{y}) = \frac{4 \nabla_{\mathbf{y}} \left[\prod_{i=1}^m |J_i(\mathbf{y})| \right]}{\prod_{k=1}^n |J_k(\mathbf{y})|}$$

For the constructed multivariate case

$$a_{kk}(\mathbf{y}) = \frac{1}{2} \left[g'(-\sqrt{y_k \bar{y}_k}) + \frac{g(\sqrt{y_k \bar{y}_k})}{\sqrt{y_k \bar{y}_k}} \right]$$

$$b_{kk}(\mathbf{y}) = \frac{y_k}{2 \bar{y}_k} \left[g'(\sqrt{y_k \bar{y}_k}) - \frac{g(\sqrt{y_k \bar{y}_k})}{\sqrt{y_k \bar{y}_k}} \right]$$

$$d_k(\mathbf{y}) = \frac{1}{\bar{y}_k} \left[\sqrt{y_k \bar{y}_k} \left[\frac{g'(\sqrt{y_k \bar{y}_k})}{g(\sqrt{y_k \bar{y}_k})} + \frac{g''(\sqrt{y_k \bar{y}_k})}{g'(\sqrt{y_k \bar{y}_k})} \right] - 1 \right]$$

and all other values of $a_{ij}(\mathbf{y})$ and $b_{ij}(\mathbf{y})$ are zero for $i \neq j$.

For the few examples studied, good performance results were not obtained with this test. However, it was by observing the form of this test and what role each term played that the approximate solution used in the text was arrived at. This is why this test is outlined in this Appendix.

REFERENCES

[A1] J. Capon, "On the Asymptotic Efficiency of Locally Optimum Detectors," *IRE Trans Inf. Theory* IT-7, 67-71 (1961).

[A2] A.B. Martinez, P.F. Swaszek, and J.B. Thomas, "Locally Optimal Detection in Multivariate Non-Gaussian Noise," *IEEE Trans. Inf. Theory* IT-30(6), 815-822 (1984).

Appendix B VARIANCE CALCULATIONS

After substituting the expression for $g^{-1}(\xi)$ for Weibull clutter into the integral for the variance, it becomes

$$\sigma_y^2 = \frac{M_y^2}{2\sigma_x^2} \int_0^\infty \left(\frac{\xi}{\sqrt{2 \ln 2}} \right)^{4/\alpha} \xi \exp - (\xi^2 / 2\sigma_x^2) d\xi.$$

Using the change of variable

$$n = \frac{1}{2} \xi^2$$

and setting $\sigma_x = 1$,

$$\sigma_y^2 = \frac{M_y^2}{2} (\ln 2)^{-2/\alpha} \int_0^\infty n^{2/\alpha} e^{-n} dn$$

The integral is the gamma function, $\Gamma\left(\frac{2}{\alpha} + 1\right)$ equal to $(2/\alpha) \Gamma(2/\alpha)$, and the desired result is obtained.

After substituting the expression for $g^{-1}(\xi)$ for lognormal clutter into the integral for the variance, it becomes

$$\sigma_y^2 = \frac{M_y^2}{2\sigma_x^2} \int_0^\infty \exp \left[\sqrt{2} \sigma_l \operatorname{erf}^{-1} (1 - 2 \exp - (\xi^2 / 2\sigma_x^2)) \right] \exp - (\xi^2 / 2\sigma_x^2) d\xi$$

Using the change of variable

$$\eta = 2 \exp - \xi^2 / 2$$

and $\sigma_x = 1$,

$$\sigma_y^2 = \frac{M_y^2}{4} \int_0^2 \exp \left[\sqrt{2} \sigma_l \operatorname{erf}^{-1} (1 - \eta) \right] d\eta$$

Changing variable again with

$$\tau = \sqrt{2} \sigma_l \operatorname{erf}^{-1} (1 - \eta)$$

and

$$\eta = 1 - \operatorname{erf}^2 (\tau / 2\sigma_l),$$

and noting the differential relationship

$$d \operatorname{erf}^2 (\tau / 2\sigma_l) = \sqrt{\frac{2}{\pi \sigma_l^2}} (\exp - (\tau^2 / 2\sigma_l^2)) d\tau,$$

then

$$\sigma_y^2 = \frac{M_y^2}{4} \int_{-\infty}^{\infty} \exp \left[\sqrt{2} \sigma_l \operatorname{erf}^{-1} (1 - \eta) \right] \sqrt{\frac{2}{\pi \sigma_l^2}} (\exp - (\tau^2 / 2\sigma_l^2)) d\tau.$$

B. CANTRELL

After completing the square,

$$\sigma_y^2 = \frac{M_y^2}{2} \exp(\sigma_l^2/2) \left[(1/(\sqrt{2\pi} \sigma_l)) \int_{-\infty}^{\infty} \exp - \frac{1}{2} \left(\frac{\tau - \sigma_l^2}{\sigma_l} \right)^2 d\tau \right].$$

The remaining integral defined in the bracket is one leaving the result in the text.

Appendix C CORRELATION COEFFICIENT CALCULATION

Substituting for $g^{-1}(\cdot)$ in the integral,

$$\rho_y(k) = \frac{M_y^2}{\sigma_y^2} \int_0^\infty \int_0^\infty \frac{(2 \ln 2 \sigma_x^2)^{-2/\alpha}}{\sigma_x^4 (1 - \rho_x^2(k))} \xi_l^{\left[\frac{2}{\alpha} + 1\right]} \xi_{l+k}^{\left[\frac{2}{\alpha} + 1\right]} \\ \times I_1 \left[\frac{\rho_x(k) \xi_l \xi_{l+k}}{\sigma_x^2 (1 - \rho_x^2(k))} \right] \exp - \left[\frac{\xi_l^2 + \xi_{l+k}^2}{2\sigma_x^2 (1 - \rho_x^2(k))} \right] d\xi_l d\xi_{l+k}.$$

Using the change of variables

$$\mu^2 = \xi_l^2 + \xi_{l+k}^2 \\ n^2 = 2\xi_l \xi_{l+k}$$

and their inverses

$$\xi_l = \frac{1}{2} \sqrt{\mu^2 + n^2} + \frac{1}{2} \sqrt{\mu^2 - n^2} \\ \xi_{l+k} = \frac{1}{2} \sqrt{\mu^2 + n^2} - \frac{1}{2} \sqrt{\mu^2 - n^2}$$

the integral can be written as

$$\rho_y(k) = \frac{M_y^2 (2 \ln 2 \sigma_x^2)^{-2/\alpha}}{\sigma_y^2 \sigma_x^2} \int_0^\infty \int_0^\infty \frac{(n^2/2)^{\frac{2}{\alpha} + 1} n \mu}{\sigma_x^2 (1 - \rho_x^2(k)) \sqrt{n^2 - \mu^2}} \\ \times I_1 \left[\frac{\rho_x(k) n^2}{2\sigma_x^2 (1 - \rho_x^2(k))} \right] \exp - \left[\frac{\mu^2}{2\sigma_x^2 (1 - \rho_x^2(k))} \right] d\mu dn.$$

Changing variables again,

$$w = \frac{\mu^2}{2\sigma_x^2 (1 - \rho_x^2(k))} \\ \Lambda = \frac{n^2}{2\sigma_x^2 (1 - \rho_x^2(k))}$$

the integral can be written as

$$\rho_y(k) = \frac{M_y^2 (2 \ln 2)^{-2/\alpha} (1 - \rho_x^2(k))^{2/\alpha + 1}}{2\sigma_y^2} \int_0^\infty \Lambda^{\frac{2}{\alpha} + 1} I_0(\mu_x(\Lambda)) \\ \times \left[e^{-\Lambda} \int_0^\infty \frac{e^{-w}}{\sqrt{w(w + 2\Lambda)}} dw \right] d\Lambda.$$

The integral in the bracket is the zeroth order Bessel function of the first kind, and can be found on page 316 of Ref. [5]. The remaining integral is

$$\int_0^\infty \Lambda^{\frac{2}{\alpha} + 1} I_0(\mu_x(\Lambda)) d\Lambda$$

This integral is equal to

$$2^{2/\alpha} \rho_v(k) \Gamma^2 \left[\frac{1}{\alpha} + \frac{3}{2} \right] F \left[\left[\frac{1}{\alpha} + \frac{3}{2} \right], \left[\frac{1}{\alpha} + \frac{3}{2} \right], 2, \rho_v^2(k) \right]$$

as shown on page 693 in Ref. [5]. Substituting for σ_v , the relationship between $\rho_v(k)$ and $\rho_s(k)$ is

$$\begin{aligned} \rho_v(k) &= \left[\frac{\alpha}{2} \right] \rho_s(k) (1 - \rho_s^2(k))^{2/\alpha + 1} \left[\Gamma^2 \left[\frac{1}{\alpha} + \frac{3}{2} \right] / \Gamma \left[\frac{2}{\alpha} \right] \right] \\ &\times F \left[\left[\frac{1}{\alpha} + \frac{3}{2} \right], \left[\frac{1}{\alpha} + \frac{3}{2} \right], 2, \rho_s^2(k) \right]. \end{aligned}$$

Appendix D IMPORTANCE SAMPLING

The importance-sampling procedure [D1,D2] is a Monte Carlo technique that distorts the generation of the random number so that the events of interest occur more frequently than, but in the same manner as, the events occur in nature. The probability of the event occurring is then compensated with a weighting factor so that the true probability of the event is obtained.

To compute the probability density of the detector, the filter values are quantized by

$$\lambda = m\Delta\lambda \text{ where } m = 0, \dots, M-1.$$

The probability density is computed by

$$p(\lambda \text{ is between } (m-1)\Delta\lambda \text{ and } m\Delta\lambda) = \frac{1}{N} \sum_{k=1}^N \delta_k$$

where N is the number of Monte Carlo samples and $\delta_k = 1$ if no importance sampling is used. The equation is simply counting the percentage of time the samples fall in the m th interval. For importance sampling,

$$\delta_k = \frac{|R_{x_d}|}{|R_{x_t}|} \exp - \frac{1}{2} \left\{ \bar{x}_t' R_{x_t}^{-1} x_t - \bar{x}_d' R_{x_d}^{-1} x_d \right\}$$

where R_{x_d} and R_{x_t} are the covariance matrixes under distortion and no-distortion and x_d and x_t are the values of the random samples generated under distortion and no-distortion. Let σ_d^2 and σ_t^2 be the variances under distortion and no-distortion. Under these conditions,

$$R_{x_t} = \sigma_t^2 \begin{bmatrix} 1 & \rho_x(1) \\ \rho_x(1) & 1 \end{bmatrix},$$

$$R_{x_d} = \sigma_d^2 \begin{bmatrix} 1 & \rho_x(1) \\ \rho_x(1) & 1 \end{bmatrix},$$

and

$$L_d = \begin{bmatrix} \sigma_d & 0 \\ \sigma_d \rho_x(1) & \sigma_d \sqrt{1 - \rho_x^2(1)} \end{bmatrix}$$

where the L_d matrix is used instead of L in generating the random samples.

REFERENCES

- [D1] F.S. Hillier and G.J. Lieberman, *Introduction to Operations Research* (Holden-Day, San Francisco, 1967), pp. 457-459.
- [D2] B.H. Cantrell and G.V. Trunk, "Corrections to 'Angular Accuracy of a Scanning Radar Employing a Two Pole Filter,'" *IEEE Trans. Aerospace and Electronic Systems* AES-10(6), 878-881 (1974).